

# COMPARISON OF THE AURORAL ELECTRON PRECIPITATIONS IN THE NORTHERN AND SOUTHERN CONJUGATE REGIONS BY TWO DMSP SATELLITES

K. MAKITA\*, C.-I. MENG

*Applied Physics Laboratory, The Johns Hopkins University,  
Laurel, Maryland 20707, U.S.A.*

and

S.-I. AKASOFU

*Geophysical Institute, University of Alaska, Fairbanks, Alaska 99701, U.S.A.*

**Abstract:** The electron precipitation in the northern and southern conjugate regions, observed by the DMSP-F2, F3 and F4 satellites, is examined. The high energy auroral electron precipitation region (the average energy higher than 500 eV and the number flux greater than  $10^7$  electrons/cm<sup>2</sup>·s·sr) shows similar electron precipitation patterns in the conjugate regions, regardless of the degree of geomagnetic activity. On the other hand, the width and structure of the low energy auroral electron precipitation regions (the average energy lower than 500 eV and the number flux greater than  $10^7$  electrons/cm<sup>2</sup>·s·sr) during quiet periods are somewhat different in the opposite hemispheres. Some of the differences seem to be controlled by the interplanetary magnetic field.

## 1. Introduction

The similarity of auroral displays in the northern and southern conjugate regions has been discussed by many authors in the past (DEWITT, 1962; BELON *et al.*, 1969; DAVIS *et al.*, 1971; STENBAEK-NIELSEN *et al.*, 1972; MAKITA *et al.*, 1981). In this respect, a fortunate opportunity has arisen to examine the degree of similarity of auroral electron precipitations in the conjugate regions, since two DMSP satellites, DMSP-F2 and F3, transversed occasionally through the northern and southern conjugate auroral regions, respectively, nearly simultaneously. These satellites had low altitude (~840 km) sun-synchronous circular polar orbits along the dawn-dusk meridian and carried identical auroral electron detectors for energies ranging from 50 eV to 20 keV. These data are also supplemented by DMSP-F4 satellite data. Further information about the satellites and detectors can be found in HARDY *et al.* (1979).

In describing the DMSP data, it is important to recall that WINNINGHAM *et al.* (1975) showed that there are two distinct regions of electron precipitations which are associated with the central plasma sheet (CPS) and the boundary plasma sheet (BPS), respectively. These two precipitation regions can also be identified in the DMSP electron data, and we shall examine the conjugacy of these two regions in terms of the

---

\* On leave from Takushoku University, 4-14, Kohinata 3-chome, Bunkyo-ku, Tokyo 112.

electron number flux (electrons/cm<sup>2</sup>·s·sr), the energy flux (ergs/cm<sup>2</sup>·s·sr) and the average energy (keV) for different degrees of geomagnetic activity.

This is a progress report on our investigation of characteristics of the auroral electron precipitations in the conjugate areas.

## 2. Results

We present first three typical conjugate electron precipitation events observed during a quiet, a moderately disturbed and a disturbed period, respectively, and then show the average electron precipitation pattern in both hemispheres during extremely quiet times and examine their conjugacy.

### 2.1. Case study

Figure 1 shows an example of the electron precipitations observed in both hemispheres during an extremely low geomagnetic activity. On the left hand side of the diagram, the top panel illustrates the *AE* index and the arrow indicates approximately

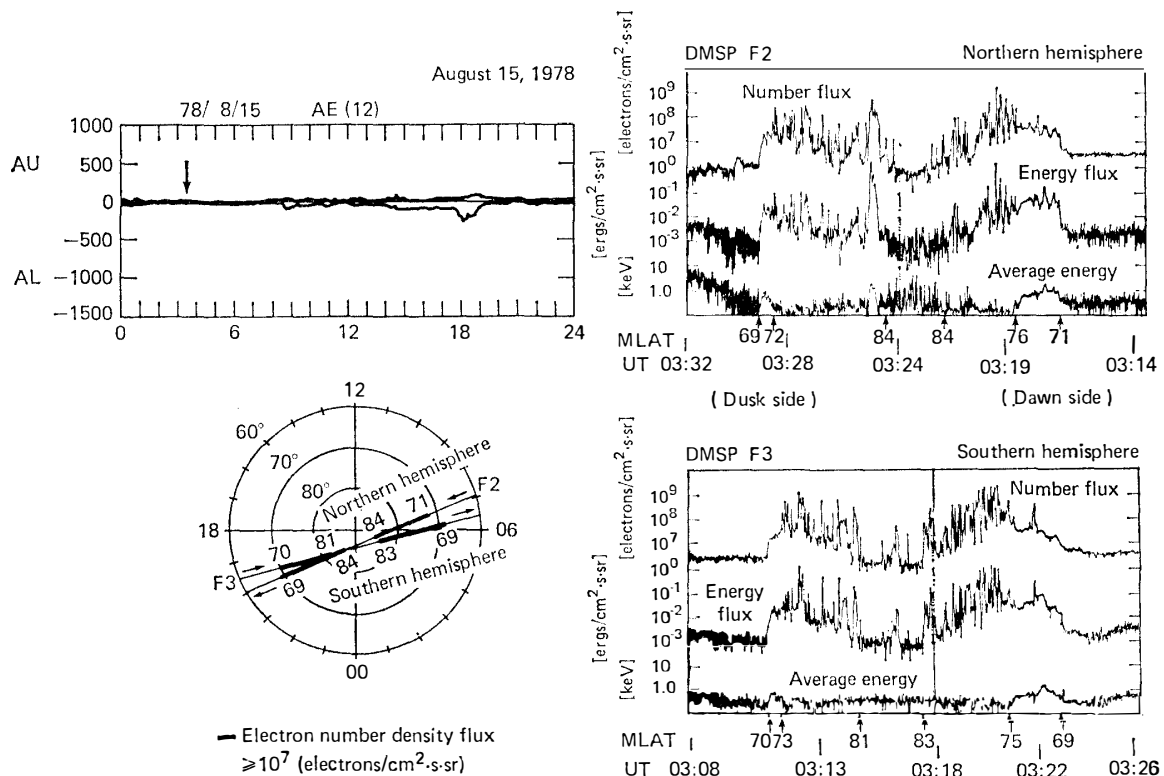


Fig. 1. An example of electron precipitation observed by two satellites in opposite hemispheres during extremely quiet time. Top left panel illustrates the *AE* index and the arrow indicates the time when the satellites pass through the polar regions. Bottom left panel shows two satellite trajectories over the conjugate polar regions in the geomagnetic latitude and local time coordinates and thick line represents the enhanced electron precipitation region. Right two panels show the electron number flux, energy flux and average energy observed at opposite hemispheres. DMSP-F2 satellite traversed the polar region along dawn to dusk direction in the northern hemisphere and DMSP-F3 satellite traversed in the reversal direction from dusk to dawn in the southern hemisphere. Note the width of electron precipitation in dusk side is somewhat different in opposite hemispheres.

the time when the two satellites passed over the polar regions. It is clear that there was no substorm activity for several hours before these particular passes; the *AE* index was very low (less than 50 nT). The left bottom panel shows the trajectories of the two satellites over the conjugate polar region in geomagnetic latitude and local time coordinates, and the heavy line segments correspond to the regions of enhanced electron precipitations ( $>10^7$  electrons/cm<sup>2</sup>·s·sr). The two panels on the right side show the electron number flux, the energy flux and the average energy observed in both hemispheres. The DMSP-F2 satellite traversed the northern polar region along the dawn-to-dusk direction between 0314 and 0332 UT and the DMSP-F3 satellite traversed the southern polar region in the reversal direction, namely along the dusk-to-dawn direction, between 0308 and 0326 UT. It can be seen that the precipitations with the average energy greater than 500 eV are similar in both hemispheres. On the right hand side, the electron precipitations observed by the two satellites are shown. In the dusk sector, the region of the enhanced electron number flux and the average energy greater than  $10^7$  electrons/cm<sup>2</sup>·s·sr and 500 eV, respectively, are located from 69° to 72° in the northern hemisphere and from 70° to 73° in the southern hemisphere. Thus, the precipitation patterns of electrons with the average energy greater than 500 eV are similar in the conjugate regions. The enhanced electron precipitations with the average energy less than 500 eV are located in the higher latitude side, from 72° to 84° in the northern hemisphere and from 73° to 81° in the southern hemisphere. Thus, the width of soft electron precipitations is somewhat different in the two hemispheres. It is 12° wide in the northern hemisphere and 8° wide in the southern hemisphere.

On the other hand, in the dawn sector, the enhanced electron precipitation with the average energy greater than 500 eV can be seen from 71° to 76° in the northern hemisphere and from 69° to 75° in the southern hemisphere. Thus, the width of the high energy electron precipitation is about 5° wide in the northern hemisphere and 6° in the southern hemisphere. In the higher latitude side, the enhancement of electron precipitation with the average energy less than 500 eV can be seen from 76° to 84° in the northern hemisphere and 75° to 83° in the southern hemisphere. Thus, the width of the low energy electron precipitation is about 8° wide in both hemispheres. Therefore, the latitudinal extent of electron precipitations of the dawn side polar region is similar in both hemispheres.

As shown in Fig. 1, there are two distinct electron precipitation regions: one of them can be seen in the lower latitude part of the auroral oval, and its average energy is higher than 500 eV. Hereafter, this region is called the high energy auroral electron precipitation region. The other region can be seen in the higher latitude part of the auroral oval, and its average electron energy is lower than 500 eV. This region is called the low energy auroral electron precipitation region. These regions will be described in detail later in the statistical study.

Figure 2 illustrates the distribution of electron precipitations in both hemispheres during a quiet period between two magnetospheric substorms. The DMSP-F3 satellite traversed the northern polar region from the morning sector to the evening sector between 0920 to 0936 UT, and the DMSP-F2 satellite traversed the southern polar region from the evening to the morning sector between 0922 to 0940 UT. The geomagnetic condition can be inferred from the *AE* index inserted in Fig. 2.

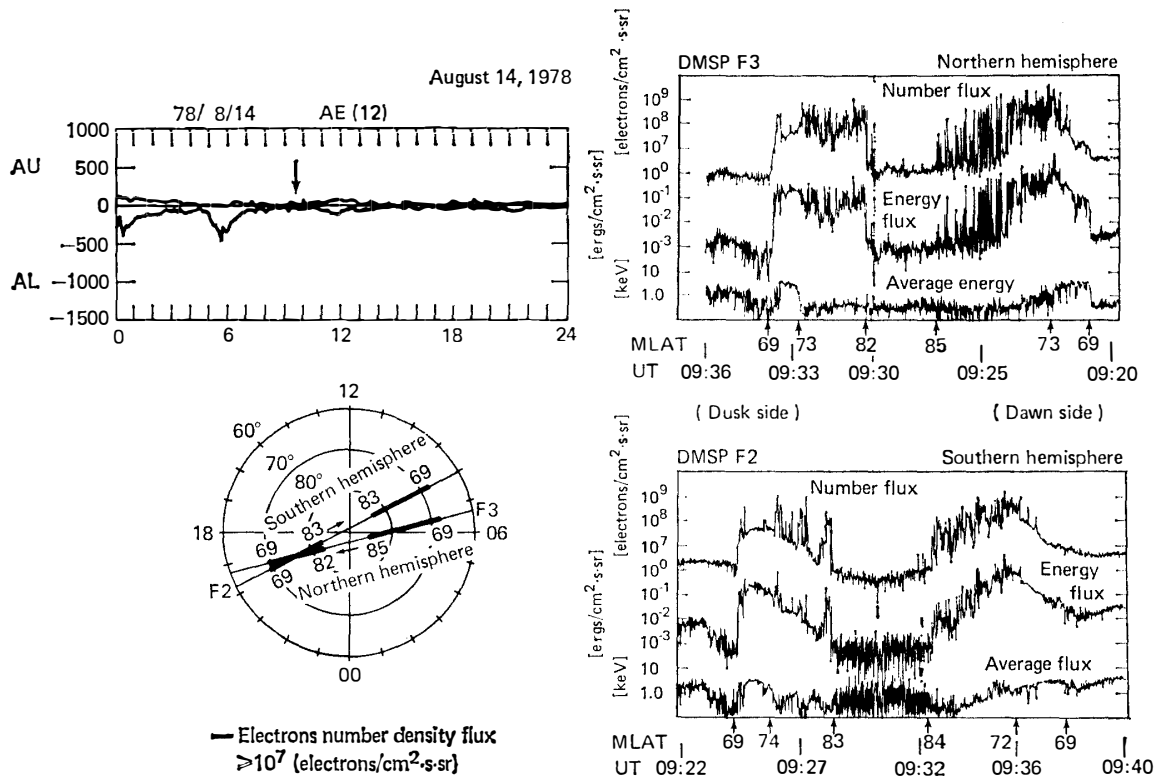


Fig. 2. An example of electron precipitation observed by two satellites in opposite hemispheres during quiet time between magnetospheric substorms. The format of the presentation is the same as that in Fig. 1. Note that the fine structure of electron precipitations in dusk side are somewhat different between the opposite hemispheres.

In the dusk sector, the high energy auroral electron precipitation regions can be found from  $69^\circ$  to  $73^\circ$  in the northern hemisphere and from  $69^\circ$  to  $74^\circ$  in the southern hemisphere. The width and the location of the two high energy auroral electron precipitation regions are similar in both hemispheres. The low energy auroral electron precipitation regions can be found from  $73^\circ$  to  $82^\circ$  in the northern hemisphere and from  $74^\circ$  to  $83^\circ$  in the southern hemisphere. Thus, the width of the low energy auroral electron precipitations in the dusk sector is similar in both hemispheres. However, fine structures of the electron precipitations in the two hemispheres are different. For example, the intensity and the energy flux in the dusk sector are fairly uniform over the entire magnetic latitude region from  $73^\circ$  to  $82^\circ$  in the northern polar region, but irregular in the southern hemisphere.

In the dawn sector, the enhanced high and low energy auroral electron precipitation regions can be found from  $69^\circ$  to  $73^\circ$  and  $73^\circ$  to  $85^\circ$ , respectively, in the northern hemisphere and from  $69^\circ$  to  $72^\circ$  and  $72^\circ$  to  $84^\circ$ , respectively, in the southern hemisphere. Thus, the width of both high and low energy auroral electron precipitation regions in the dawn sector is nearly the same in both hemispheres.

Figure 3 shows an example which illustrates the conjugacy of electron precipitations during a high geomagnetic activity period. The intense magnetospheric substorm ( $AE \sim 650$  nT) took place two hours before this particular observing time, and this conjugate polar crossing took place during the recovery phase (the  $AE$  index  $\sim 500$  nT).

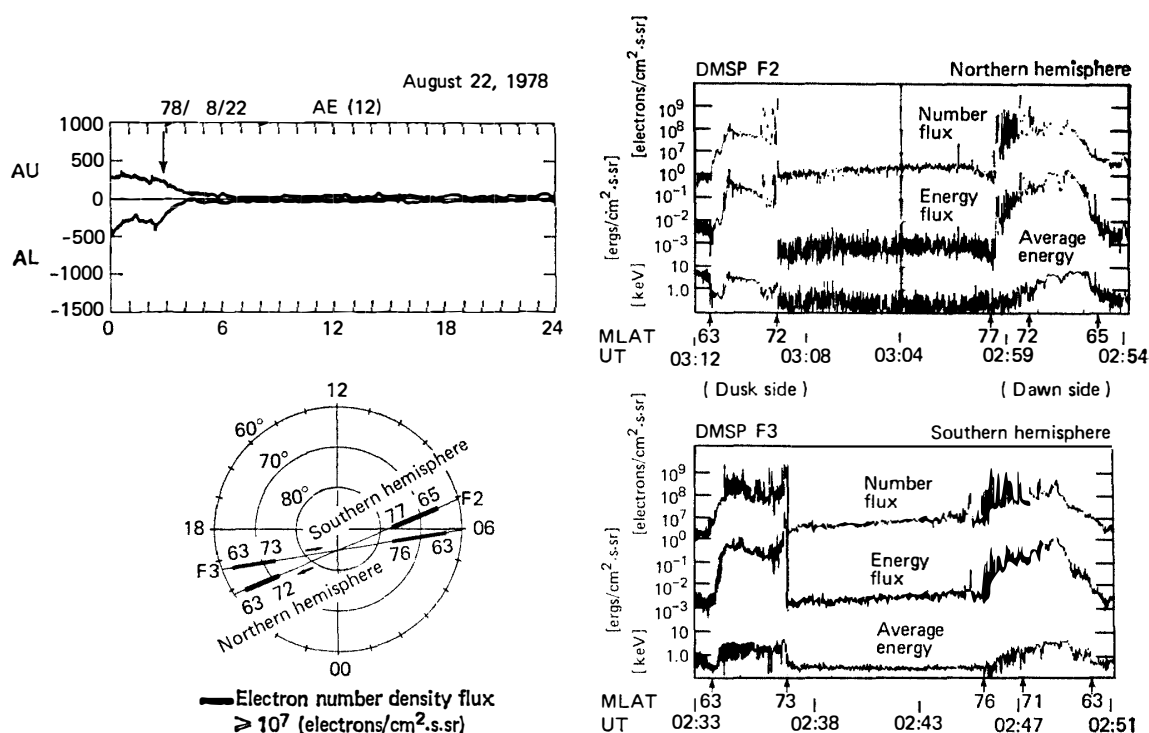


Fig. 3. An example of electron precipitation observed by two satellites in opposite hemispheres during the high activity period of recovery phase. The format of the presentation is the same as that in Fig. 1. Note that the width and location of electron precipitation in both dawn and dusk sectors are very similar between both hemispheres.

The DMSP-F2 satellite traversed the northern polar region from 0254 to 0312 UT while the DMSP-F3 satellite traversed the southern polar region from 0233 to 0251 UT. Obviously, the average energy of electron precipitations during disturbed periods is higher than that of quiet periods; see the previous examples. The high and low energy auroral electron precipitation regions are now defined as the average energy above or below 1 keV, instead of 500 eV during the quiet periods.

In the dusk sector, the high energy auroral electron precipitation region was detected from  $63^{\circ}$  to  $72^{\circ}$  in the northern hemisphere and from  $63^{\circ}$  to  $73^{\circ}$  in the southern hemisphere. The dusk low energy auroral electron precipitation region could not be identified in either hemisphere. In the dawn sector, the high energy electron precipitation region was located from  $65^{\circ}$  to  $72^{\circ}$  in the northern hemisphere and from  $63^{\circ}$  to  $71^{\circ}$  in the southern hemisphere. The low energy auroral electron precipitation region can be found from  $72^{\circ}$  to  $77^{\circ}$  in the northern hemisphere and from  $71^{\circ}$  to  $76^{\circ}$  in the southern hemisphere. Therefore, this event shows that the width and location of the high and low energy auroral electron precipitations in both dawn and dusk sector are similar between the two conjugate regions. We examined also some other events during high geomagnetic activity periods and found that this similarity in the conjugate auroral regions is common.

## 2.2. Statistical study

In order to learn a little more about the average electron precipitation patterns in both polar regions, we made a statistical study of the precipitation patterns. Since the

amount of data during disturbed periods are not sufficient for our statistical study at the present time, we examined only the electron precipitation pattern in both hemispheres during low geomagnetic activity. We selected all available events from the DMSP-F2, F3 and F4 satellites during extremely quiet conditions, defined by the  $AE$  index less than 100 nT and  $Kp$  index less than 1+. There are 349 passes over the northern polar region and 453 passes over the southern polar region during the period between January 1978 and December 1979, which satisfied the above selection criterion of extremely quiet conditions.

We examined the location of the equatorward boundary, the high and low energy transition boundary and the poleward boundary of the enhanced electron precipitations for all selected events which covered all local time sectors. The equatorward edge is defined by the lowest latitude of the region where the electron number flux is greater than  $10^7$  electrons/cm<sup>2</sup>·s·sr. This boundary is likely to correspond to the equatorward boundary of the auroral oval. The transition boundary is defined by the change in the average energy from 500 eV to higher or lower energies. The structure of the precipitation changes also near the transition boundary, from a fairly uniform, continuous type to a more burst type (WINNINGHAM *et al.*, 1975). The poleward boundary is defined by the high latitude edge of the soft precipitation region with fluxes greater than  $10^7$  electrons/cm<sup>2</sup>·s·sr and the average energy lower than 500 eV; this definition can reasonably well distinguish the polar cap from the auroral oval. However, the poleward boundary position is often difficult to determine definitively due to large fluctuations in both the electron number flux and the energy flux associated with the occurrence of discrete auroral arcs. In this report, the poleward boundary of the auroral electron precipitation is identified by the highest latitude edge of the continuous electron precipitation region without a dip to the background level. In this way, isolated spikes are automatically excluded. As illustrated by Fig. 1, the high energy auroral electron precipitation region during extremely quiet times is characterized by its narrow width and minor fluctuating spatial structures, while the low energy auroral electron precipitation region is very wide with large fluctuating structures.

Figure 4a and 4b show the average location of these three boundaries in the northern and southern hemispheres. The data are subgrouped into the following four magnetic local time sectors: 03 to 09, 09 to 15, 15 to 21 and 21 to 03 MLT. The magnetic latitude of the average location of equatorward, transition and poleward boundaries are shown in each sector. The standard deviations from the average values and the number of samples used in each sector are also shown.

Comparing the average locations of these boundaries, one can see that both the average high energy auroral electron precipitation region and the average low energy auroral electron precipitation region are very similar in the conjugation regions. The high energy auroral electron precipitation region is rather narrow, and its width is 3° in the midnight sector (21 to 03 MLT), about 4° in the evening sector (15 to 21 MLT) and about 5° in both the morning (03 to 09 MLT) and noon sectors (09 to 15 MLT). On the other hand, the low energy auroral electron precipitation region is rather wide, about 12° in the midnight sector, about 10° in the evening sector and about 9° in the morning and noon sectors.

We also examined the electron precipitation region during extremely quiet periods

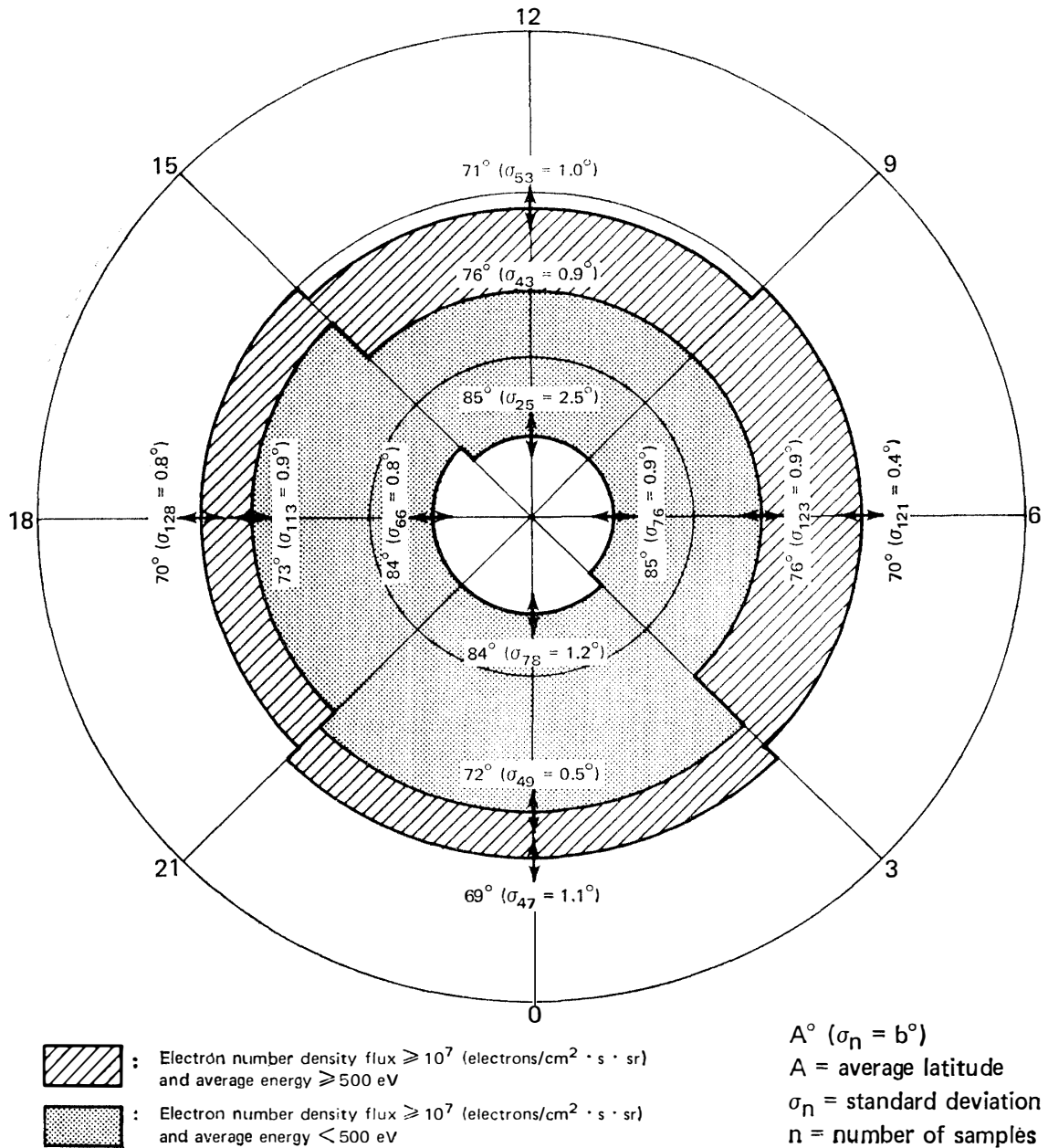


Fig. 4a. Average electron precipitation pattern in northern hemisphere for all seasons in 1978 and 1979 during extremely quiet times ( $AE < 100$  nT,  $Kp < 1+$ ). The data are sub-grouped into four sectors according to their magnetic local time, 03 to 09, 09 to 15, 15 to 21 and 21 to 03 MLT. The magnetic latitude of the average equatorward, transition and poleward boundaries are shown in each sector. The standard deviation of the average latitude of each boundary and the number of samples examined in this analysis are also shown.

in the local summer and winter seasons. It is our finding that the electron precipitation region in the noon sector (09 to 15 MLT) shows clear difference between the two seasons. For example, in the local summer hemisphere, the high energy auroral electron precipitation region in the noon sector extends, on the average, from 72° to 78°, while the low energy auroral sector extends, on the average, from 72° to 78°, while the low energy auroral electron precipitation region is located from 78° to 85°. In the local

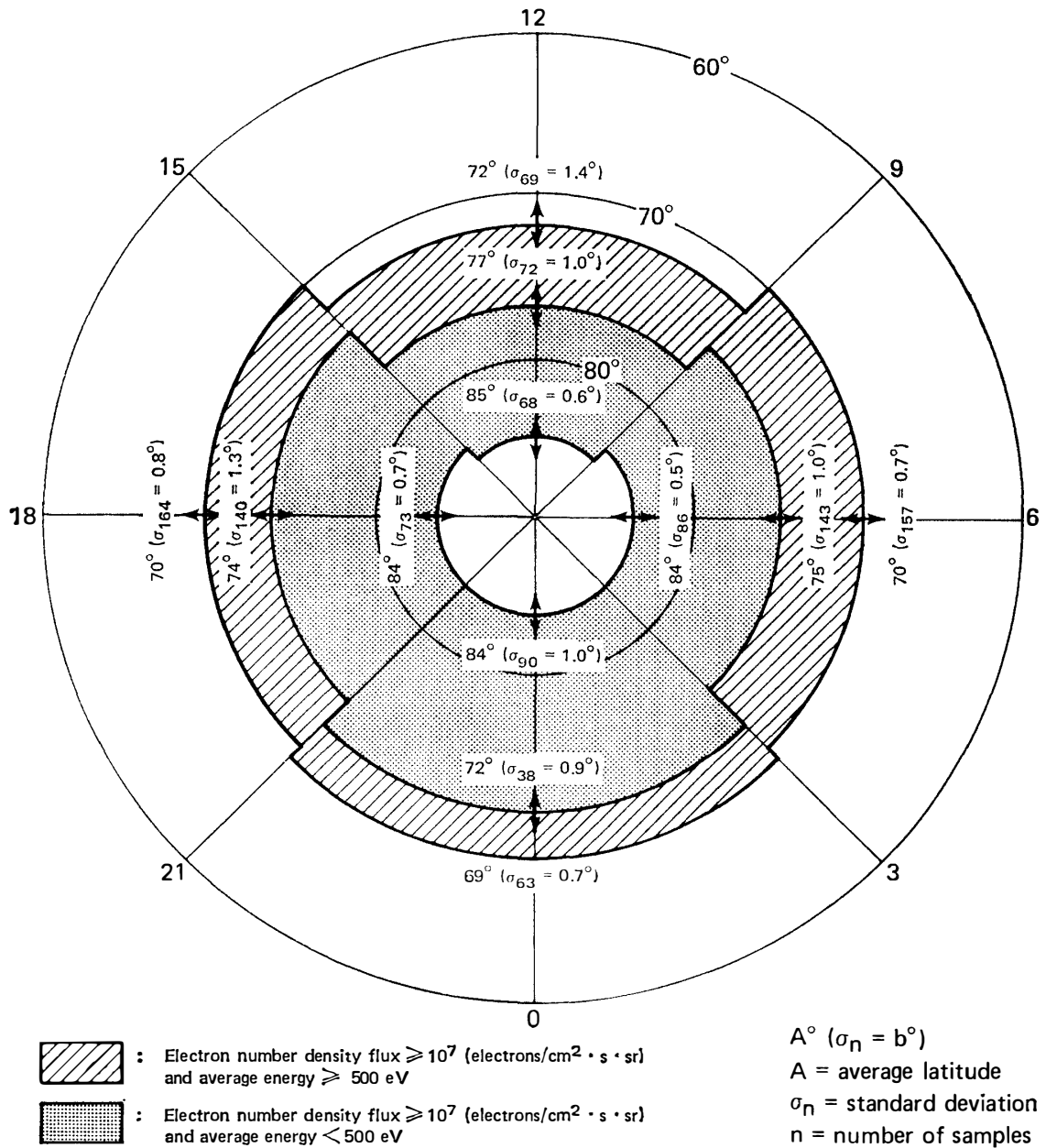


Fig. 4b. Average electron precipitation pattern in southern hemisphere for all seasons in 1978 and in 1979 during extremely quiet times ( $AE < 100$  nT,  $Kp < 1+$ ). The format of the presentation is the same as that in Fig. 4a. Note that the average electron precipitation pattern in the southern hemisphere is very similar to that in the northern hemisphere.

winter hemisphere, however, the high energy auroral electron precipitation region in the noon sector is from 70° to 76° and the low energy auroral electron precipitation region is from 76° to 84°. Thus, this result indicates that the auroral electron precipitation region in the noon sector in the local summer hemisphere is located at a higher latitude by about 2° than that in the local winter hemisphere. But, the seasonal differences in other magnetic local time sectors cannot be clearly recognized at this time.

### 3. Discussion

From several events illustrated here and others examined, the dawn-dusk DMSP-F2 and F3 satellite observations reveal that the high energy auroral electron precipitation region, defined by the electron number flux greater than  $10^7$  electrons/cm<sup>2</sup>·s·sr with the average energy higher than 500 eV, shows a good conjugacy between the two hemispheres, both during quiet and disturbed periods. However, the width and structure of the low energy auroral electron precipitation region with the average energy lower than 500 eV are somewhat different in both hemispheres during quiet times. For example, the width of the low energy auroral electron precipitation region around the dusk sector is 12° wide in the northern hemisphere and 8° wide in the southern hemisphere, as shown in Fig. 1. Among five examined examples of the simultaneous conjugate electron precipitation during quiet period, two examples revealed that the width of low energy auroral electron precipitation region in the dusk sector is quite different between the northern and the southern hemispheres, similar to Fig. 1. In three other examples, the low energy auroral electron precipitation regions over opposite hemispheres are rather similar and their deviation is within two degrees.

Since the low energy auroral electron precipitation region in both hemispheres extends to very high geomagnetic latitudes, the configuration of this region may partly be controlled by solar wind parameters. YEAGER and Frank (1976) and MENG and KROEHL (1977) reported that the soft electron fluxes over the polar region are influenced by the interplanetary magnetic field (IMF) sector structure, resulting in a significant asymmetry between two polar cap regions. Their soft electron precipitations are called polar rain (WINNINGHAM and HEIKKILA, 1974) and its electron energy and number flux are usually rather low comparing with the auroral electron precipitation. Generally the precipitation is detected only at energies below several hundred electron volts and the electron number flux is less than  $10^7$  (electron/cm<sup>2</sup>·s·sr). Although their soft electron fluxes in the polar cap are not related to the low energy auroral electron precipitation region reported here, it may be important to examine the IMF parameters in order to understand the differences of the low energy auroral electron precipitation patterns in the conjugate regions.

According to STERN (1973), MOZER *et al.* (1974) and AKASOFU *et al.* (1981), the interconnection between the geomagnetic field and the positive IMF  $B_y$  component displaces the polar cap towards the dusk sector in the northern hemisphere and towards the dawn sector in the southern hemisphere. It is interesting to compare the IMF components during the events illustrated in this paper. The hourly average values of the IMF components for the August 15, 03 UT event (Fig. 1) are  $B=4.5$ ,  $B_x=3.0$ ,  $B_y=-2.6$  and  $B_z=0.5$  nT. Indeed, the observed skewing of the conjugate polar cap region is consistent with the earlier studies that it is caused by the negative IMF  $B_y$  component. For the August 14, 09 UT event (Fig. 2), no IMF data are available. During the disturbed period (Fig. 3), the conjugate electron precipitations were similar in both hemispheres and the corresponding hourly average values of the IMF were  $B=7.1$ ,  $B_x=4.1$ ,  $B_y=3.4$  and  $B_z=-4.4$  nT. It is not possible to determine the dawn-dusk displacement of the polar cap region associated with the  $B_y$  variation for these two examples. However, AKASOFU and ROEDERER (1982) showed that the IMF  $B_y$

asymmetry can clearly be seen only when the  $B_z$  component is positive and the magnitude  $B$  is small ( $< 3$  nT).

We examined here also the average electron precipitation pattern during extremely quiet periods in the four local time sectors by using the DMSP-F2, F3 and F4 electron data. It is found that the high energy auroral electron precipitation region and the low energy auroral electron precipitation region are very similar in the two hemispheres. For example, the average width of the high energy auroral electron precipitation region is widest (about  $5^\circ$  or  $6^\circ$ ) in both the morning sector (03 to 09 MLT) and the noon sector (09 to 15 MLT) and is narrowest (about  $3^\circ$ ) in the midnight sector (21 to 03 MLT) in both hemispheres. On the other hand, the average width of the low energy auroral electron precipitation region is widest (about  $12^\circ$ ) in the midnight sector (21 to 03 MLT) and is narrowest (about  $8^\circ$  or  $9^\circ$ ) in both the morning sector (03 to 09 MLT) and the noon sector (09 to 15 MLT) in both polar regions. MCDIARMID *et al.* (1975) examined the average electron precipitation pattern and the electron precipitation intensity at several energies during moderate geomagnetic activity periods on the basis of ISIS-2 satellite data. Comparing their results with our observations, the general characteristics of their electron precipitation pattern seems to be similar to ours, except for the fact that their low energy electron precipitation did not extend to very high latitudes. This can be attributed to the fact that our selection of data is limited only to extremely quiet periods.

We examined also the seasonal variations of the average electron precipitation pattern in both hemispheres and found that the average electron precipitation region in the noon sector extends to a higher latitude in the local summer hemisphere by about  $2^\circ$  than in the local winter hemisphere. This result is consistent with what one can expect from the seasonal variation of the geomagnetic field line configuration based on the magnetospheric model of MEAD and FAIRFIELD (1975). They showed the dayside field lines emerging at about  $78^\circ$  in local summer hemisphere, for example, anchor at about  $75^\circ$  in the local winter hemisphere during quiet times. This seasonal effect of  $3^\circ$  in the day sector is very similar to the seasonal variation of average precipitation pattern obtained here.

In order to understand the morphology of electron precipitation during extremely quiet periods in more detail, we examined also IMF effects on the electron precipitation and found that the poleward boundary of the low energy auroral electron precipitation region shifted to a higher latitude in all local time sectors as the IMF- $B_z$  component increases. However, no effects on the high energy auroral electron precipitation region by the IMF- $B_z$  component was detected in the present analysis. The IMF  $B_x$  and  $B_y$  component effects on the high and low energy auroral electron precipitation regions were also investigated, but no clear result was obtained. More events may be needed in order to reach any definitive conclusions about these problems.

### Acknowledgments

This work was supported in part by the National Institute of Polar Research in Japan and by the Air Force Office of Scientific Research Grant AFOSR-79-0010 and the Atmospheric Science Division, NSF Grant ATM-79-23240 to the Johns Hopkins

University and NSF Grant ATM-81-15321 to the University of Alaska.

### References

- AKASOFU, S. -I. and ROEDERER, M. (1982): A three-dimensional model of the magnetosphere. submitted to *Planet. Space Sci.*
- AKASOFU, S. -I., COVEY, D. N. and MENG, C. -I. (1981): Dependence of the geometry of the region of open field lines on the interplanetary magnetic field. *Planet. Space Sci.*, **29**, 803-807.
- BELON, A. E., MAGGS, J. E., DAVIS, T. N., MATHER, K. B., GLASS, N. W. and HUGHES, G. H. (1969): Conjugacy of visual auroras during magnetically quiet periods. *J. Geophys. Res.*, **74**, 1-28.
- DAVIS, T. N., HALLINAN, T. J. and STENBAEK-NIELSEN, H. C. (1971): Auroral conjugacy and time dependent geometry of auroras. *The Radiating Atmosphere*, ed. by McCORMAC. Dordrecht, D. Reidel, 160-169.
- DEWITT, R. N. (1962): The occurrence of aurora in geomagnetically conjugate areas. *J. Geophys. Res.*, **67**, 1347-1352.
- HARDY, D. A., GUSSENHOVEN, M. S. and HUBER, A. (1979): The precipitation electron detectors (SSJ/3) for the block 5D/flight 2-5 DMSP satellites: Calibration and data presentation. Rep. AFGL-TR-79-0210, Hanscom Air Force Base, Massachusetts.
- KAMEI, T. and MAEDA, H. (1981): Auroral electrojet indices (*AE*) for July-December 1978. *WDC-C2 Geomagn. Data Book*, **4**, 108 p.
- MAKITA, K., HIRASAWA, T. and FUJII, R. (1981): Visual auroras observed at the Syowa Station-Iceland conjugate pair. *Mem. Natl Inst. Polar Res., Spec. Issue*, **18**, 212-225.
- MCDIARMID, J. B., BURROWS, J. R. and BUDZINSKI, E. E. (1975): Average characteristics of magnetospheric electrons (150 eV to 200 keV) at 1400 km. *J. Geophys. Res.*, **80**, 73-79.
- MEAD, G. D. and FAIRFIELD, D. H. (1975): A quantitative magnetospheric model derived from spacecraft magnetometer data. *J. Geophys. Res.*, **80**, 523-534.
- MENG, C. -I. and KROEHL, H. W. (1977): Intense uniform precipitation of low-energy electron over the polar cap. *J. Geophys. Res.*, **82**, 2305-2313.
- MOZER, F. S., GONZALEZ, W. D., BOGOTT, F., KELLEY, M. C. and SHULZ, S. (1974): High latitude electric field and the three-dimensional interaction between the interplanetary and terrestrial magnetic field. *J. Geophys. Res.*, **79**, 56-63.
- STENBAEK-NIELSEN, H. C., DAVIS, T. N. and GLASS, N. W. (1972): Relative motion of auroral conjugate point during substorm. *J. Geophys. Res.*, **77**, 56-63.
- STERN, D. P. (1973): A study of the electric field in an open magnetospheric model. *J. Geophys. Res.*, **78**, 7292-7305.
- WINNINGHAM, J. D. and HEIKKILA, W. J. (1974): Polar cap auroral electron fluxes observed with Isis 1. *J. Geophys. Res.*, **79**, 949-957.
- WINNINGHAM, J. D., YASUHARA, F., AKASOFU, S. -I. and HEIKKILA, W. J. (1975): The latitudinal morphology of 10 eV to 10 keV electron fluxes during magnetically quiet and disturbed times in the 2100-0300 MLT sector. *J. Geophys.*, **22**, 3148-3171.
- YEAGER, D. M. and FRANK, J. A. (1976): Low energy electron intensities at large distances over the earth's polar cap. *J. Geophys. Res.*, **81**, 3966-3976.

(Received August 3, 1982; Revised manuscript received November 20, 1982)